RESIDUAL FLEXURAL PROPERTIES OF IMPACTED PPS-C AND EPOXY-C COMPOSITE LAMINATES

José Ricardo Tarpani, jrpan@sc.usp.br
Carlos do Amaral Razzino, crazzino@sc.usp.br
Maria Cristina Adami Gatti, mcgatti@sc.usp.br
Escola de Engenharia de São Carlos - EESC - USP, Departamento de Engenharia de Materiais, Aeronáutica e Automobilística, Avenida Trabalhador São-Carlense, 400, CEP 13566-590, São Carlos - SP, Brasil, Fone 16 3373 9591, Fax 16 3373 9590

Abstract. *Residual flexural properties of low-energy transversely impacted thermoplastic polyphenylene sulphide (PPS) and themosetting epoxy resin (EPX) composite laminates reinforced with continuous carbon (C) fibers, were determined. On the basis of externally observed damage created by impact loading, the PPS-C composite laminate was identified as less damage resistant than EPX-C composite, although similar energy absorbing capacities were determined for the concurrent structural materials. All quasistatic monothonic flexural properties of the laminates was negatively affected by impact loading, and decreased proportionally to the increase on impact energy. The superiority of PPS-C over EPX-C laminate has been shown for strenght and stiffness parameters in all the tested conditions, although ductility and tenacity parametes of EPX-C were somewhat higher than PPS-C composite for the virgin and impacted conditions at the lower-energy range.*

Keywords*: Polymer Composite Laminate, Impact Damage, Residual Property, Aircraft Material.*

1. INTRODUCTION

The aeronautical industry has emerged as the major and most efficient mean of transport in the modern world. Therefore, there is a high demand for new technologies to reduce its operating costs and increase its application, while decreasing the number of aircraft accidents. One of the main strategies to achieve these goals is the development of new structural materials with high strength and stiffness-to-density ratios. Thermoplastic polymer matrix composite laminates (e.g., PEEK: poly-ether-ether-ketone, PPS: polyphenylenesulphide, PEI: poly-ether-imide [1-3]) reinforced with high performance fibers (C: carbon, G: glass, Q: quartz, A: aramid) have rapidly reached the position of one of the most promising materials for the construction of sub- and supersonic commercial aircrafts, at expenses of more traditional thermosetting polymer matrix laminates [4-6].

Aircrafts are subject to a wide range of impact events during operational in-service conditions and periodical maintenance programs [7]. For composite laminates, relatively low energy impacts are particularly dangerous insofar they may remain undetected for long time periods. Impact damage compromises the structural integrity of laminated structures, especially their in-plane compression properties [8-14]. The well-known concept of barely visible impact damage-BVID deals with this subject, and generally establishes the limiting condition of 0.3 mm indentation depth [12].

For high-performance thermoplastic laminates, relatively few studies have been made regarding light impact damage; however, as for thermosetting matrix composites, delamination has been identified as the major problem due to low-energy contact under dynamic loading [9,10].

2. MATERIALS AND TEST SPECIMENS

5 mm-thick thermoplastic PPS-C laminates were fabricated by hot pressing polyphenylenesulphide semi-impregnated 3K 5HS (harness satin) bi-directional carbon fiber fabrics arranged in the stacking sequence $[(0/90), (+45/-45)_2, (0/90)]_4$. 5 mm-thick thermosetting EPX-C laminates were manufactured by vacuum bagging and autoclave curing at 180°C rubber-toughened epoxy resin pre-impregnated 3K 8HS bi-directional carbon fiber fabrics disposed according to the architecture $[(0/90), (+45/-45)_2, (0/90)]_6$. Finished laminates presented nominally 60% volume fraction of reinforcing fibers.

Full-thickness standard compression-after-impact (CAI) specimens (Figure 1) with in-plane dimensions of (100 x 150) mm^2 according to ASTM-D7136 [15] were waterjet cut from the manufactured plates.

3. EXPERIMENTAL

3.1 Impact Testing

Transverse impact testing was performed at ambient temperature in an adapted semi-instrumented Charpy testing system (Figure 2) with full-scale load capacity of 50 J, at impact velocities ranging from 1 to 3.5 m/s.

The rectangular samples were firmly attached to a frame support structure and a single impact was applied through-the-specimen-thickness direction by means of a 16 mm diameter steel ball mounted in a striker, at impact energies varying from 5 to 50 J. Typically, three specimens of both the composite laminates were tested for each energy level, and the semi-instrumented system automatically recorded the absorbed energy during the impact events.

Figure 1. Sets of CAI test specimens: (a) Thermoplastic PPS-C laminate; (b) Thermosetting EPX-C composite.

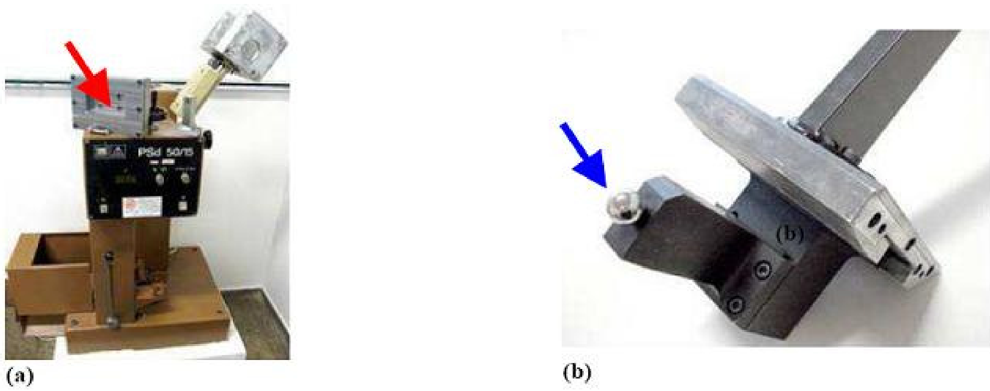

Figure 2. (a) Charpy impact testing system (the CAI specimen frame is indicated by the red arrow); (b) Impactor assembly (tup) with the 16 mm diameter steel ball indicated by the blue arrow.

The depth of the impact indentation mark left over the front surface of CAI specimens was measured with a dial gage as illustrated in Figure 3, whereas a caliper was employed to quote the indentation diameter. Typically, five indentation-depth measurements were assessed for each test specimen, while only two (orthogonally oriented) measurements were performed to determine the average diameter.

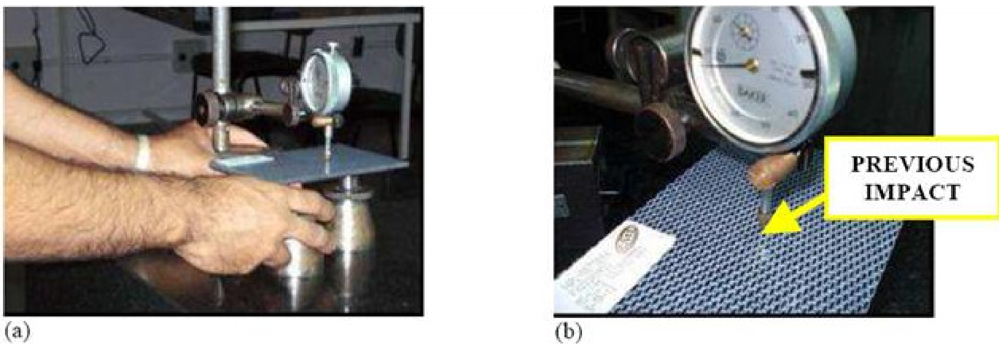

Figure 3. (a) Indentation-depth measurement in a PPS-C specimen; (b) Close view of the dial gage instrument and the impact indentation mark.

3.2 Monothonic Quasistatic Three-Point Flexure Test

Figure 4 depicts the test set-up utilized in the monothonic flexure tests of previously impacted testpieces. The distance between the specimens´ supporting rollers was 130 mm, and the steel rollers were 30 mm in diameter.

The tests were carried out in a electro-mechanical system in full-scale of 10 ton., under displacement control of the machine ram. The test speed was set at 2 mm/min, and the specimen load-point deflection data were collected by an axial extensometer especially adapted to the test jig, with a maximum displacement capacity of 13 mm, which was sufficient to bring the testpieces to catastrophic rupture.

The residual properties determined under three-point flexure (3PF) loading were the flexural strength (*FS*), modulus of elasticity (*E*), strain (e_m) and tenacity (TML_m) at maximum load.

In determining the *FS* parameter, the formulae to estimate the peak tensile stress attained at the outer lamina subject to tensile stresses under bending loading was used, as provided in ASTM-D7264 [16]:

$$FS = 3\ P_m.L\ /\ 2\ b.h^2 \qquad (1)$$

where P_m is the maximum load (N), L is span between supporting rollers (mm), b and d the specimen width (mm) and thickness (mm), respectively.

The strain at maximum load, calculated at the exact position in the laminate where *FS* was derived (i.e., outer lamina in traction at the load-line) is given by [16]:

$$e_m = 6\ \delta_m.h\ /\ L^2 \qquad (2)$$

where δ_m is the specimen deflexion at the load-line in maximum load (mm).

The Young's modulus (stiffness) was then determined according to the tangent method, as supplied in [16]:

$$E = \Delta S\ /\ \Delta e \qquad (3)$$

where ΔS (MPa) and Δe (mm/mm) are the ranges of flexural stress (Eq.1) and strain (Eq.2), respectively, corresponding to the strain range from 0.1 to 0.3%.

Finally, the tenacity parameter TML_m (MJ/m^3) was estimated by simply integrating the area under the flexural stress vs. strain curve up to the maximum load attained during the flexure test.

Figure 4. 3PF device utilized to determine the residual monotonic properties of the impacted laminates.

4. RESULTS AND DISCUSSION

4.1 Impact Testing

Figures 5 and 6 show, respectively, the front and rear sides of previously impacted PPS-C and EPX-C laminate specimens, considering two different impact energy levels. The indentation mark left by the 16 mm spherical steel ball can be clearly observed for the thermoplastic matrix laminate, although it is only barely visible at the lower energy level for the thermosetting composite. The same is observed at the rear side of the specimens. Even for the most critical impact loading condition of 50 Joules, there was no perforation (i.e., complete penetration) of the specimens.

Figure 07 plots the results obtained during the metrological inspection of the impact damage (indentation mark) impinged to the frontal surface of the thermoplastic PPS-C and thermosetting EPX-C laminates.

Good correlations are invariably seen in regard both the indentation depth and diameter with respect to the impact energy.

Figure 7a shows that the BVID energy (at 0.3 mm indentation depth [12]) of PPS-C laminate is around only 14 J, whereas for the more damage resistant EPX-C composite it is about twice that value. Probably, the more ductile nature of the thermoplastic polymer accounted for these results. Nonetheless, a more detailed study in regard to the internal damage level (i.e., through-the-thickness damage quantification), and more importantly, the qualification of operating failure mechanisms in both composite laminates is mandatory in order to correctly appraise their impact performance.

Figure 8 plots the results of absorbed energy for both the composite laminates. Considering the data fitting curves of Figure 8a, one can conclude that thermoplastic matrix composite consumes more energy than the thermosetting matrix laminate for impacts of up to approximately 25 J, while an inverse behavior is found above that energy level. Anyway, as shown in Figure 8b, the energy absorption capacity of both the materials is remarkable, with the energy absorption ratios achieving more than 80% of the available energy for the most critical impact loading conditions.

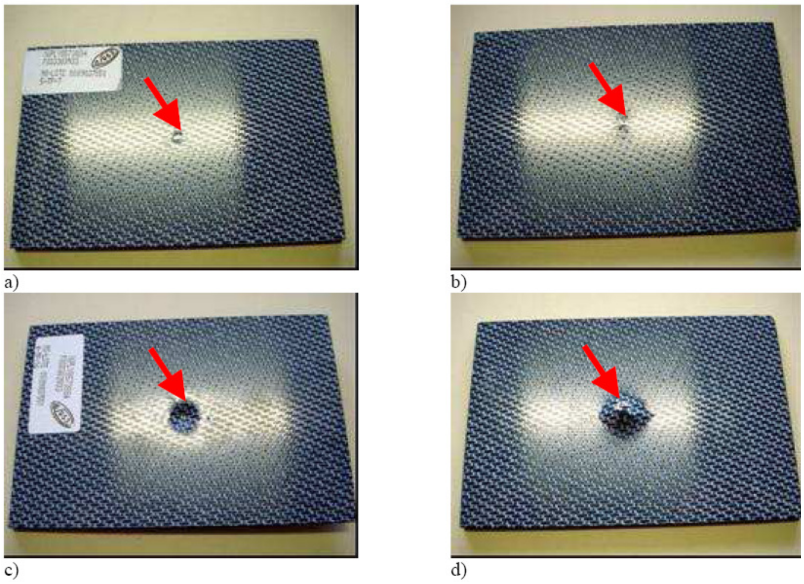

Figure 5. (a,c) Front, and (b,d) rear sides of transversely impacted PPS-C specimens at energies of: (a,b) 10 Joules; (c,d) 50 Joules.

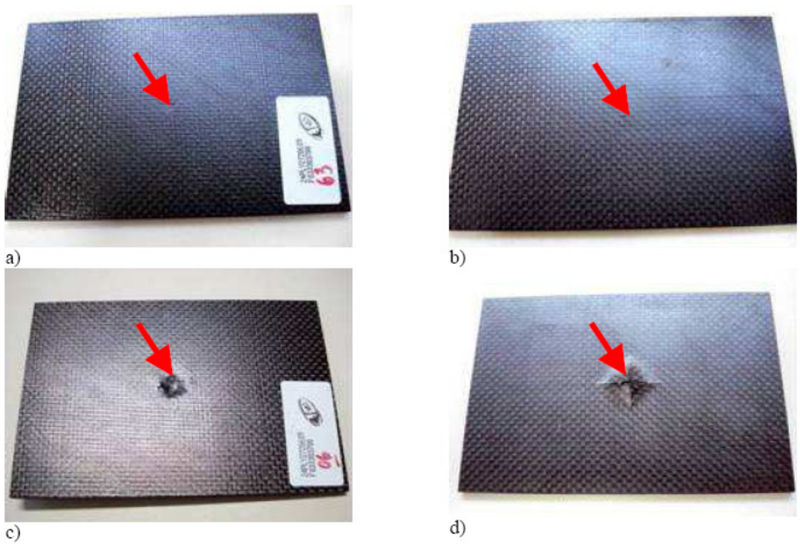

Figure 6. (a,c) Front, and (b,d) rear sides of transversely impacted EPX-C specimens at energies of: (a,b) 10 Joules; (c,d) 50 Joules.

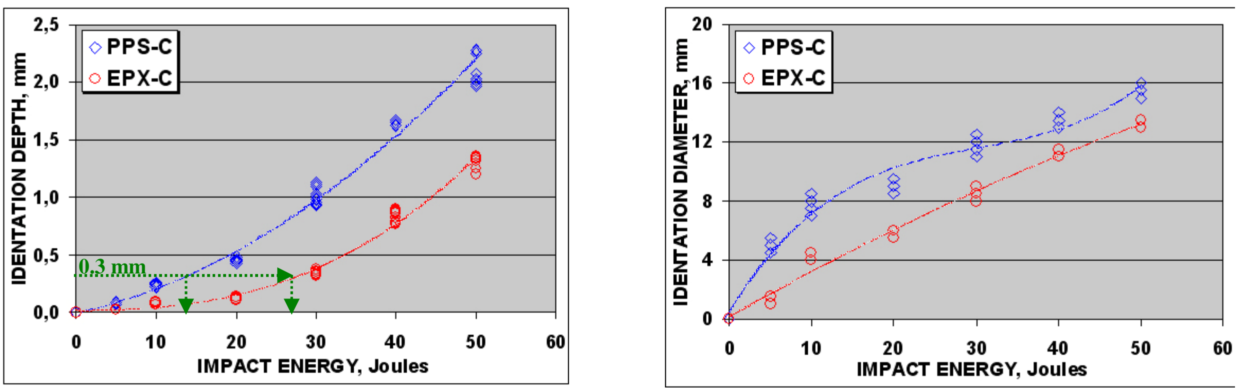

(a) (b)

Figure 7. Metrological values of the damage created by single impact in the PPS-C and EPX-C laminates as a function of the impact energy: (a) Depth of indentation; (b) Diameter of the indentation.

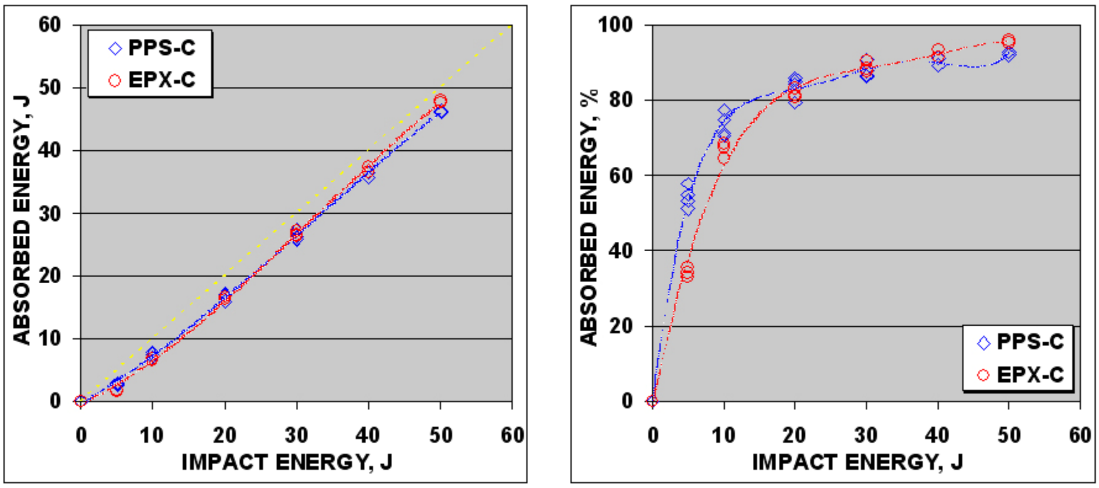

(a) (b)

Figure 8. Impact absorbed energy by the PPS-C and EPX-C laminates: (a) Absolute values; (b) Percentage basis in regard to the available impact energy.

4.2 Monothonic Quasistatic Flexure Tests

Figures 9 and 10 present the stress-strain behaviors of pristine and impacted PPS-C and EPX-C laminates. The effect of the increasing impact energy in reducing the maximum stress withstood by the specimen (i.e., its residual flexural strength) is clearly noticed. There is also a noticeable reduction of the laminate stiffness (i.e., slope of the linear elastic portion of the curves) as the impact energy is increased.

Bearing in mind that the flexural strength of the laminates is impaired due to the previously applied impact loading, one can expect that the tenacity at maximum load, which is basically the area under the stress-strain curve until that peak point, is to be also negatively affected by the dynamic loading. It is especially true if one consider the natural trend of lessening the strain at maximum load with the increment of the impact energy, as shown in Figures 9 and 10.

Figures 11 and 12 show, respectively, the front face and the longitudinal section of CAI specimens bent until fracture after previous impact. It is observed that the laminates fail essentially due to bending (i.e., mixed tensile and compression fractures), with delamination of PPS-C composite (Fig.11) occurring preferentially next to the lower (outer) beam subjected to pure tensile stresses. In the EPX-C laminate (Fig.12) there is a tendency of delamination development at the neutral plane (maximum shear stress plane) for the low energy impacted specimen, but the delamination plane is displaced to the tensile stress dominating (lower) beam as a result of the higher impact damage, which induces delamination at that position.

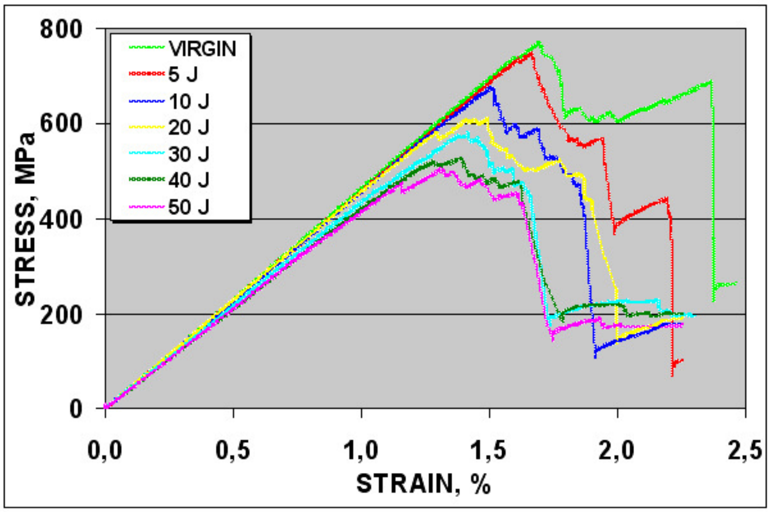

Figure 9. Stress-strain curves derived from 3PF tests of unimpacted and impacted PPS-C laminates.

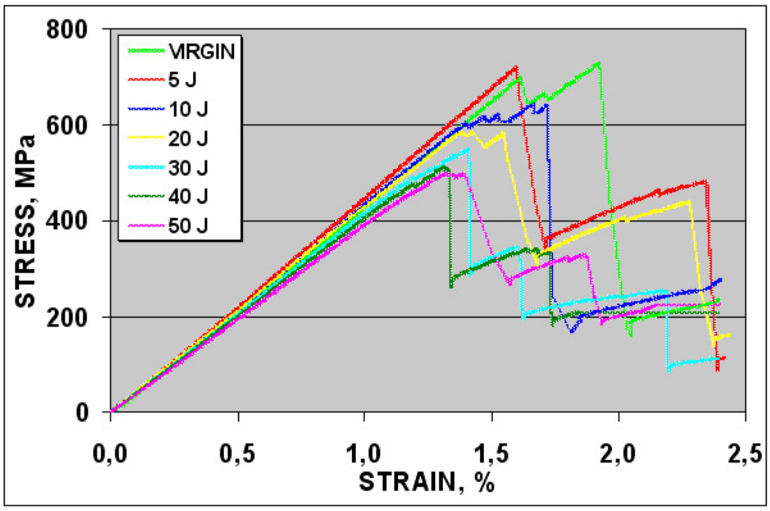

Figure 10. Stress-strain curves obtained during 3PF tests of unimpacted and impacted EPX-C laminates.

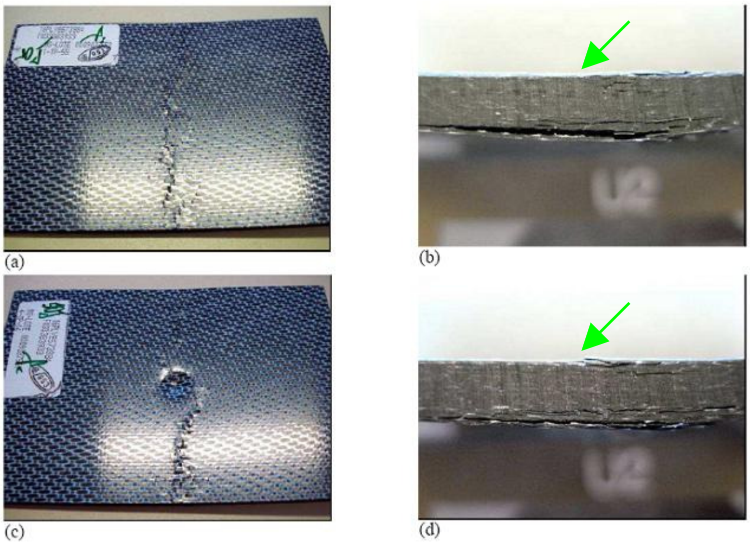

Figure 11. Front and side views of PPS-C specimens tested in 3PF after a single impact event with energy of: (a, b) 10 Joules; (c, d) 50 Joules. Arrows point out the impacted surface of the CAI specimen, which was submitted to compressive stresses during the flexure test.

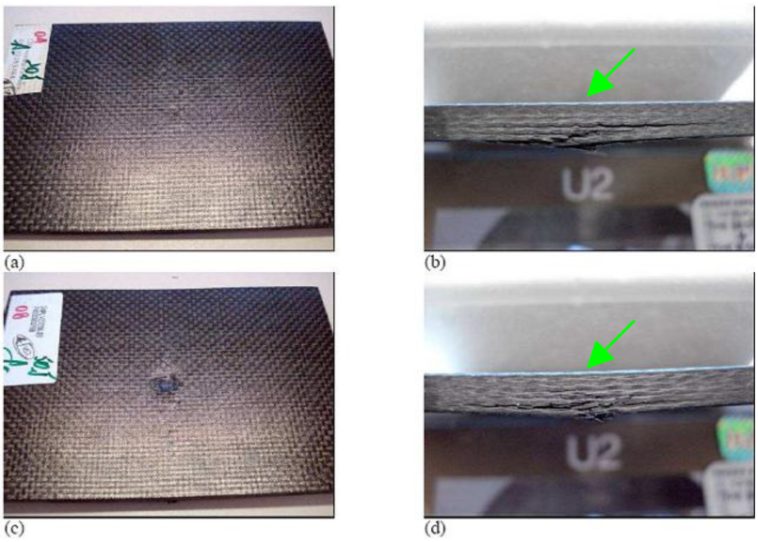

Figure 12. Front and side views of EPX-C specimens tested in 3PF after a single impact event with energy of: (a, b) 10 Joules; (c, d) 50 Joules. Arrows point out the impacted surface of the CAI specimen, which was submitted to compressive stresses during the flexure test.

Figures 13-16 compare the residual mechanical performance of PPS-C and EPX-C laminates in 3PF tests. As expected from previous analysis of Figures 9 and 10, all the mechanical properties are deteriorated by previous impact loading, decreasing proportionally to the increase on impact energy.

In general, it can be concluded that the PPS-C laminate performs significantly better than EPX-C composite, and this is particularly evident in regard to both the flexural strength and stiffness properties.

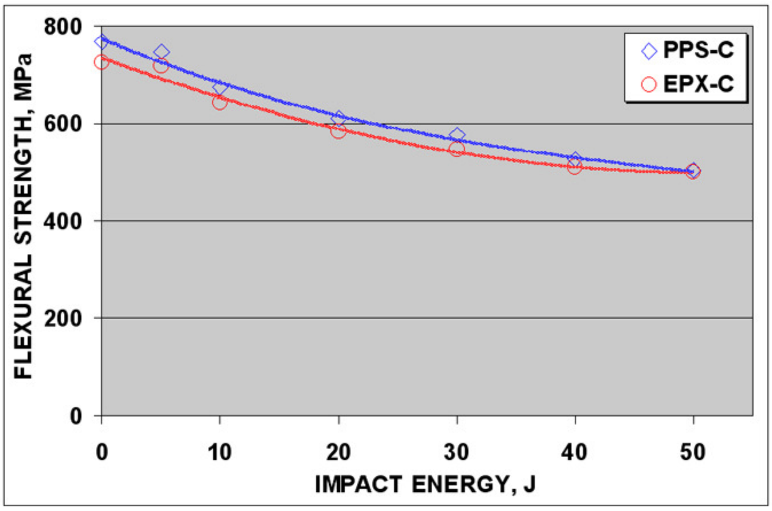

Figure 13. Ultimate flexural strength of PPS-C and EPX-C laminates as a function of the impact energy.

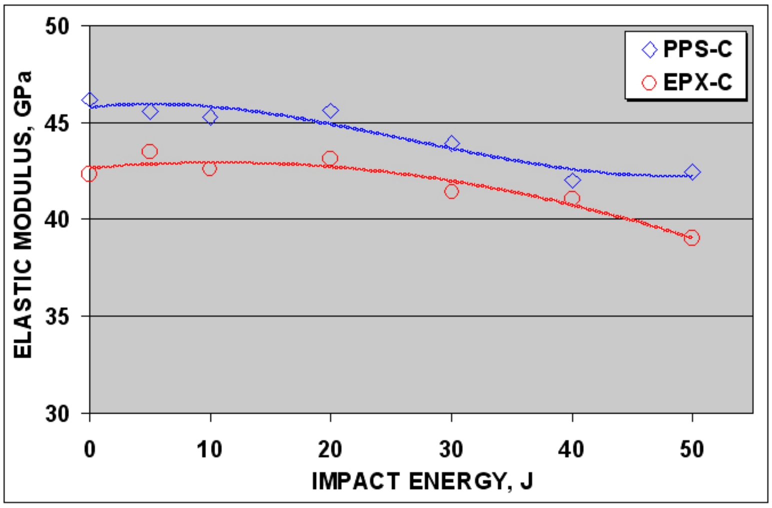

Figure 14. Flexural stiffness of PPS-C and EPX-C laminates as a function of the impact energy.

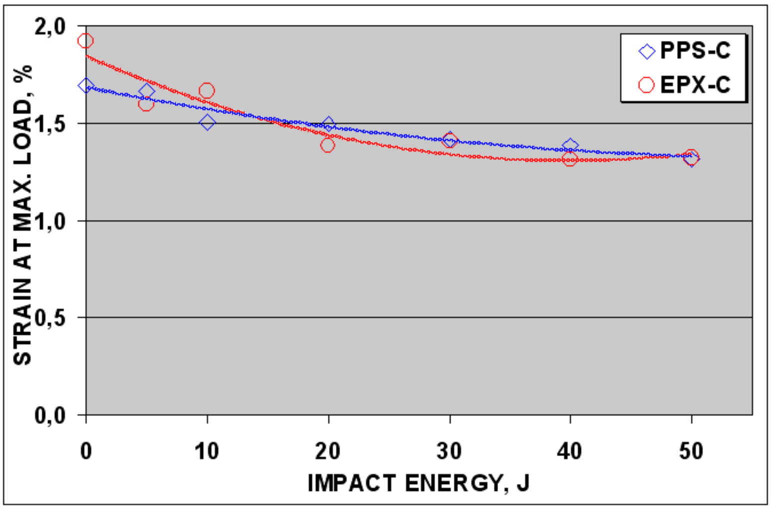

Figure 15. Flexural strain at maximum load of PPS-C and EPX-C laminates as a function of the impact energy.

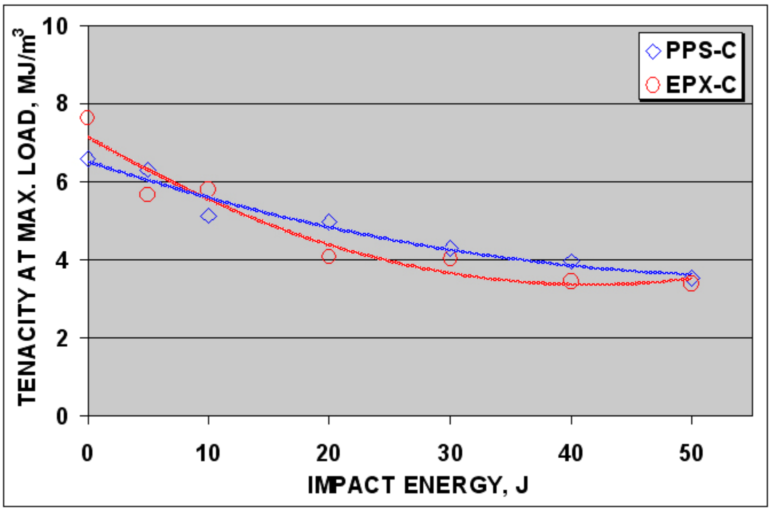

Figure 16. Flexural tenacity at maximum load of PPS-C and EPX-C laminates as a function of the impact energy.

5. CONCLUSIONS

Regarding the impact tests, the (visually detected) damage resistance of PPS-C laminate was substantially poorer than EPX-C composite, although the impact energy absorption capacities of the concurrent structural materials were virtually identical. At the most critical impact loading levels, the energy absorption ratio of both materials exceeded 90% of the available impact energy. With respect to the monothonic quasistatic flexure tests, it was observed that all mechanical properties were negatively affected by the dynamic loading, and decreased proportionally to the increase on impact energy. In general, PPS-C laminate performed significantly better than EPX-C composite, especially concerning the strength and stiffness parameters, inasmuch as high strength and stiffness are typical features of thermoplastic PPS material.

6. ACKNOWLEDGEMENTS

To Fapesp for the financial support (Proc.06/50110-3), to CNPq for the grants to the participants of the research work, and to Embraer S/A for the testpieces supplied.

7. REFERENCES

1. Corrigan E., Leach D., McDaniels T. (2001) “The influence of processing conditions on the properties of PEEK matrix composites”, ICI Advance Materials, Private Communication.
2. Maher J. (1995) “Polyphenilenesulfide: high-temperature performer”, Advanced Materials & Processes, ASM International, v.5, p.35-37.
3. Findes R.E., Bartolomucci J.P. (1996), Polyetherimides offer strength and stiffness, Advanced Materials & Processes, ASM International, v.1, p.47.
4. Hou M., Ye L., Mai Y.M. (1997) “Manufacturing process and mechanical properties of thermoplastic composite components”, Journal of Materials Processing Technology, v.63, p.334-338.
5. Díaz J., Rubio L. (2003) “Developments to manufacture structural aeronautical parts in carbon fibre reinforced thermoplastic materials”, Journal of Materials Processing Technology, v.143-144, p.342-346.
6. Fernández A., Blas F., Frövel M. (2003) “Autoclave forming of thermoplastic composite parts”, Journal of Materials Processing Technology, v.143-144, p. 266-269.
7. Alves M., Chaves C.E., Birch R.S. (2003) “Impact on aircraft”, 15° Congresso Brasileiro de Engenharia Mecânica, São Paulo-SP, Brasil.
8. Nejhad M.N.G., Parvizimajidi A. (1990) “Impact behavior and damage tolerance of woven carbon fiber reinforced thermoplastic composites”, Composites, v.21, p.155-168.
9. Jang B.P., Huang C.T., Hsieh C.Y. (1991) “Repeated impact failure of continuous fiber reinforced thermoplastic and thermoset composites”, Journal of Composite Materials, v.25, p.1171-1203.
10. Curson A.D., Leach D.C., Moore D.R. (1992) “Impact failure mechanisms of carbon fiber thermoplastic composites”, Plastics Rubber and Composites Processing and Applications, v.17, p.133-139.
11. KargerKocsis J., Yuan Q., Mayer J. (1997) “Transverse impact behavior of knitted carbon-fiber fabric-reinforced thermoplastic composite sheets”, Journal of Thermoplastic Composite Materials, v.10, p.163-172.

12. Freitas M., Reis L. (1998) “Failure mechanisms on composite specimens subjected to compression after impact”, Composite Structures, v.42. p. 365-373.
13. Datta S., Krishna A.V., Rao R.M.V.G.K. (2004) “Low velocity impact damage tolerance studies on glass-epoxy laminates - effects of material, process and test parameters”, Journal of Reinforced Plastics and Composites, v.23, p.327-345.
14. Sugun B.S., Rao R.M.V.G.K. (2004) “Low-velocity impact characterization of glass, carbon and Kevlar composites using repeated drop tests”, Journal of Reinforced Plastics and Composites, v.23, p.1583-1599.
15. ASTM-D7136M (2005) “Standard test method for measuring the damage resistance of a fiber-reinforced polymer matrix composite to a drop-weight impact event”, American Society for Testing and Materials, West Conshohocken, Pennsylvania.
16. ASTM-D7264M (2007) “Standard test method for flexural properties of polymer matrix composite materials”, American Society for Testing and Materials, West Conshohocken, Pennsylvania.

8. RESPONSIBILITY NOTICE

The authors are the only responsible for the printed material included in this paper.